Catalysis Today 142 (2009) 239–244

Contents lists available at ScienceDirect

Catalysis Today

journal homepage: www.elsevier.com/locate/cattod

Influence of the V + Mo/Al ratio on vanadium and molybdenum speciation and catalytic properties of V–Mo–ZSM-5 prepared by solid-state reaction

M. Mhamdi [a,*], A. Ghorbel [a], G. Delahay [b]

[a] Laboratoire de Chimie des Matériaux et Catalyse, Département de Chimie, Faculté des Sciences de Tunis, 2092 Tunis, Tunisia
[b] Institut Charles Gerhardt Montpellier, UMR 5253, CNRS-UM2-ENSCM-UM1, Eq. "Matériaux Avancés pour la Catalyse et la Santé", ENSCM (MACS-Site la Galéra), 8 rue Ecole Normale, 34296 Montpellier Cedex 5, France

ARTICLE INFO

Article history:
Available online 7 September 2008

Keywords:
Solid-state exchange
Vanadium
Molybdenum
Zeolite
NO-SCR by NH_3

ABSTRACT

V–Mo–ZSM-5 catalysts with various composition prepared by solid-state ion exchange were investigated with respect to their physico-chemical characteristics using chemical analysis, XRD, BET, DRIFT, UV–vis, ^{27}Al MAS-NMR spectroscopy, H_2 TPR and TPD of NH_3. It was found that all the preparations leads to either metal ions sitting at the bridging oxygen of Si–OH–Al or anchored at Si–OH groups or deposited as oxide. These different solids were tested in the selective catalytic reduction of NO_x by ammonia. The main result is that upon addition of small amount of Mo to V–ZSM-5, catalytic performances were enhanced.

1. Introduction

Transition metals can be introduced into zeolite via impregnation, decomposition of metal organic complex or ion exchange. Ion exchange can be carried out in liquid solution or by solid-state exchange reaction, which consists of heating a mixture of two powders, one being the zeolite and the other the active phase salt precursor, so as to induce thermally the diffusion of the salt into the zeolite [1,2]. The solid-state exchange offers a number of advantages than the conventional exchange of zeolites since it avoids handling of large volume of salt solution and the problem of how to discharge waste salt solution. Furthermore, it is possible to obtain a high degree of exchange by one step and solvatation does not play any role.

NO_x emissions from both mobile and stationary sources are a problem of great concern nowadays, and several methods were proposed in order to meet the current NO_x legislation emission limits. In the case of stationary sources, the selective catalytic reduction of NO_x by ammonia is to date considered the best available technology, being able to reduce NO_x emission at ppm levels. In fact, commercial SCR monolith catalysts are made up by an anatase TiO_2 carrier that supports the active compnents, i.e., vanadium and tungsten (or molybdenum). Vanadia is active in the reduction of NO_x but also in the undesired oxidation of SO_2 to SO_3; accordingly the V_2O_5 content is generally low (2%, w/w). WO_3 or MoO_3 are employed in much larger amounts and they act as both a "chemical" and "structural" promoter, i.e.; they increase the reactivity of V_2O_5/TiO_2 catalysts by enlarging the temperature window of the SCR reaction and improves the mechanical, structural, and morphological properties of the catalysts [3–5]. Catalysts contyaining MoO_3 instead of WO_3 are also employed in industrial practice, they have been reported to be less active but more tolerant to poisoning compounds [6]. However, the use of TiO_2 as support is limited by the fact that is posses low resistance to sintering, low surface area and high cost. Therfore, to improve their performances, many supporters have been used [7,8]. The aim of this work is to study the effect of the molar ratio of V + Mo/Al on the physico-chemical properties of vanadium and molybdenum loaded H-ZSM-5 catalysts and their catalytic performance in SCR of NO_x by ammonia.

2. Experimental

2.1. Catalysts preparation

H-ZSM-5 zeolite (Zeolyst, Si/Al = 15) was used as starting material. Solid-state exchange samples were prepared in two steps. First, powders of zeolite and ammonium metavanadate NH_4VO_3 in a desired ratio (1 or 2 wt%), were finely ground and mixed in a mortar for 15 min in ambient conditions. The resulting mixture was then heated in a helium flow (25 mL min^{-1}) up to 500 °C (heating rate: 2 °C min^{-1}) and left at 500 °C overnight (12 h). Then the obtained solid was finely ground and mixed with acetylacetonate of molybdenum in the desired molar ratio (V + Mo/Al = 2/3; 1; 4/3;

* Corresponding author. Tel.: +216 97 703 884; fax: +216 71 885 008.
E-mail address: mourad.mhamdi@gmail.com (M. Mhamdi).

0920-5861/$ – see front matter © 2008 Elsevier B.V. All rights reserved.
doi:10.1016/j.cattod.2008.07.026

2) and heated again for 12 h at 500 °C in helium. Finally the catalysts were calcined in oxygen during 1 h at 500 °C. Herein, V–Mo–ZSM-5 catalysts are identified as V*X*–Mo*Y*–Z, where *X* means vanadium content (wt%), *Y* the V + Mo/Al molar ratio and Z the parent zeolite.

2.2. Catalyst characterization

Chemical analyses were performed by ICP at the Vernaison Center of Chemical Analysis of the CNRS. XRD patterns were obtained on a diffractometer with a copper anode. Scan was taken at 2θ rate of 0.2 °/min and structural data for reference compounds were taken from the ASTM X-ray powder data file. N_2-BET analysis and porosity measurements were done on a Micrometrics ASAP 2000 apparatus at liquid nitrogen temperature. Temperature-programmed desorption of ammonia (NH_3-TPD) and temperature-programmed reduction by H_2 (H_2-TPR) were performed with a Micromeritics AutoChem 2910 apparatus.

Samples were characterized by FTIR spectroscopy with a PerkinElmer (Spectrum BX) spectrometer using KBr pressed disks as matrices. The DRIFT experiments were carried out with a Bruker IFS 55 spectrometer equipped with a Thermo Spectra Tech reacting cell.

UV–vis diffuse reflectance spectra were recorded on a PerkinElmer Lambda 45 spectrophotometer equipped with a diffuse reflectance attachment. Solid-state MAS NMR measurements were carried out using a Bruker ASX300 spectrometer (210 MHz).

2.3. Catalytic reactions

The performances of the catalysts in the selective catalytic reduction of NO by NH_3 were evaluated as reported by Delahay and colleagues [9].

3. Results and discussion

3.1. Elemental analysis

The different catalysts were all first characterized by elemental analysis (Table 1). Two series were prepared: (i) V1–MoY–Z with 1 wt% vanadium and (ii) V2–MoY–Z with 2 wt% vanadium. The values obtained for Si, Al, Mo and V fit both the data provided by the zeolite manufacturer and the expected nominal vanadium and molybdenum loading. Thus, it confirms that no molybdenum or vanadium is lost during the solid-state reaction. All the metals loaded are either on the external surface of the zeolite crystals or diffused inside its channels.

3.2. BET surface area and porosity

In Table 1 are reported the main textural characteristics of the zeolites and vanadium–molybdenum catalysts, including surface area, microporous volume and total porous volume, measured by N_2 physisorption as a function of the zeolite topology. Nitrogen adsorption/desorption isotherms on ZSM-5 and V–Mo–Z are very similar and close to a type I characteristic of microporous materials, although the V–Mo-catalysts show small hysterisis loop at higher partial pressures, which reveals some intergranular mesoporosity. As can be seen from Table 1, BET surface area, microporous and porous volumes, decrease after the introduction of molybdenum and vanadium in zeolite indicating a textural alteration which can be induced by the presence of oxide aggregates, small polymolybdate or alumino-molybdate species that partially block both the pore inside or at the enter of channels of the zeolite.

3.3. X-ray diffraction

XRD patterns of the H-ZSM-5 and V–Mo–ZSM-5 catalysts show the typical diffraction peaks at $2\theta = 22–25°$ which clearly indicated that the framework of the H-ZSM-5 was still retained without obvious changes of relative crystallinities for both V–Mo–Z series up to a Mo content lower than 10 wt%. This result suggests that the metal species (i.e. oxide, cations,...) are well dispersed through the zeolites structure and the absence of bulk phases in the XRD patterns implies that for these samples the molybdenum and vanadium oxides are present in either at nanocrystalline state or as small crystallites which measured less than 4 nm in diameter. Furthermore, XRD and FTIR (1500–400 cm^{-1}) showed no significant damage of the zeolite host structure after exchange and thermal treatment. For higher molybdenum contents, V2–Mo2–Z and V1–Mo2–Z samples, significant diffraction peaks are observed at $2\theta = 13.2$, 25.7, 27.3 which reveal the presence of large MoO_3 aggregates.

3.4. FTIR (KBr)

Fig. 1 shows the FTIR spectra of the samples after metal loading in the range 400–1000 cm^{-1}. Upon introduction of higher metal content mainly an absorption band in the range 900–910 cm^{-1} assigned to stretching vibration of $Si–O^-M^+$ linkage was observed [10]. This is generally considered to be a proof of the incorporation of the heteroatom into the framework. According to previous data the weak band in the range 900–910 cm^{-1} is assigned to terminal Mo = O in tetrahedral molybdate species attached to the surface like $(O_3Mo = O)^{2-}$ [11].

3.5. DRIFT spectroscopy

The FTIR spectra of the parent H-ZSM-5 zeolite and the V–Mo–ZSM-5 catalysts prepared are compared in Fig. 2. On the parent H-ZSM-5 zeolite bands at 3745 cm^{-1} attributed to terminal hydroxyl groups Si–OH [12,13], 3662 cm^{-1} attributed to hydroxyl groups on

Table 1
The composition of V–Mo–ZSM-5 samples

Catalysts	V (wt%)	Mo (wt%)	Si (wt %)	Al (w%)	Si/Al	S_{BET} (m^2/g)	$V_{\mu p}$[a] (cm^3/g)	V_p[b] (cm^3/g)
H-ZSM-5	–	–	36.73	2.15	16.40	340	0.118	0.261
V1–Mo2/3–Z	0.94	4.38	35.74	2.10	16.41	271	0.118	0.204
V1–Mo1–Z	1.06	7.29	34.83	2.05	16.38	213	0.084	0.176
V1–Mo4/3–Z	1.04	9.54	32.55	1.90	16.51	231	0.085	0.173
V1–Mo2–Z	1.03	14.47	31.27	1.87	16.12	112	0.046	0.079
V2–Mo2/3–Z	1.96	2.82	36.43	2.10	16.72	297	0.101	0.225
V2–Mo1–Z	2.05	5.93	35.04	2.23	15.15	222	0.080	0.195
V2–Mo4/3–Z	1.95	8.42	33.67	2.18	14.89	164	0.070	0.151
V2–Mo2–Z	2.01	13.11	31.10	1.99	15.07	160	0.060	0.130

[a] $V_{\mu p}$: microporous volume.
[b] V_p: porous volume.

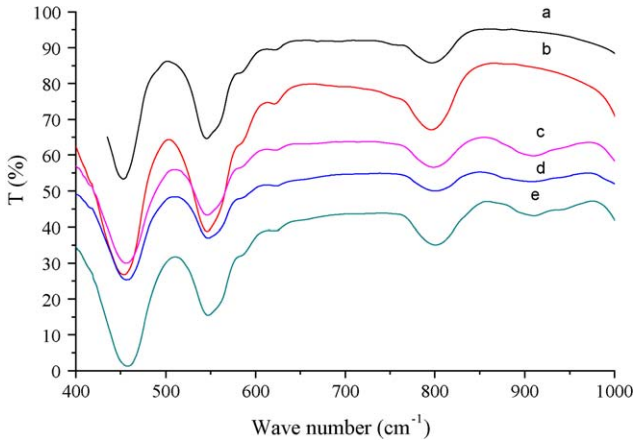

Fig. 1. (a) H-ZSM-5; (b) V2–Z; (c) Mo1–Z; (d) V1–Mo1–Z; (e) V2–Mo1–Z.

extra framework aluminium [14] and 3609 cm^{-1} assigned to strong Brönsted acid sites Si–OH–Al [12,13,15] were observed. The comparison of the spectra of parent zeolite and the samples issued from solid-state exchanged shows that the intensity of the bands assigned to strong Brönsted acid sites (Si–OH–Al) and that attributed to bridging silanols Si–OH underwent a great decrease after metal loading. This result suggests that the V and Mo ions are mainly located at the bridging oxygen of Si–OH–Al groups as tetrahedral monomers MoO_4 or dimmers Mo_2O_7 as suggested by [16,17] but also grafted on Si–OH sites. Obviously, a part of this decrease may be due to physical covering of hydroxyls groups by oxide species.

3.6. TPD of ammonia

The amount of ammonia desorbed from the catalysts and the maximum temperature of desorption are summarized in Table 2. For the parent H-ZSM-5, two peaks at 211 and 420 °C can be observed in the NH_3-TPD profile (Fig. 3), assigned to desorption of NH_3 from weak [18] and strong Brønsted acid sites [19,20], respectively. NH_3-TPD profiles obtained on the different prepared samples confirm that during the solid-state reaction, the area of the high temperature peak corresponding to the strong Brønsted acid sites decreased considerably. This result indicates that the vanadium and molybdenum species spreads and diffuses into the channels and preferentially interact with the strong Brønsted acid sites of ZSM-5 and that anchoring takes place by exchanging with the acidic H atoms. The vanadium and molybdenum species inside the channel of ZSM-5 consume the strong Brønsted acid sites which consequently decrease with increasing metal loading. At the same time, the l-peak shifts to higher temperature as the acid sites of medium strength increase (Table 2). The NH_3 TPD profiles of the V–Mo–Zeolite samples show a decrease of high temperature peak surface after molybdenum loading. This result may be explained by the lowering of the amount of Brönsted acid sites due to interaction between Mo and V ions.

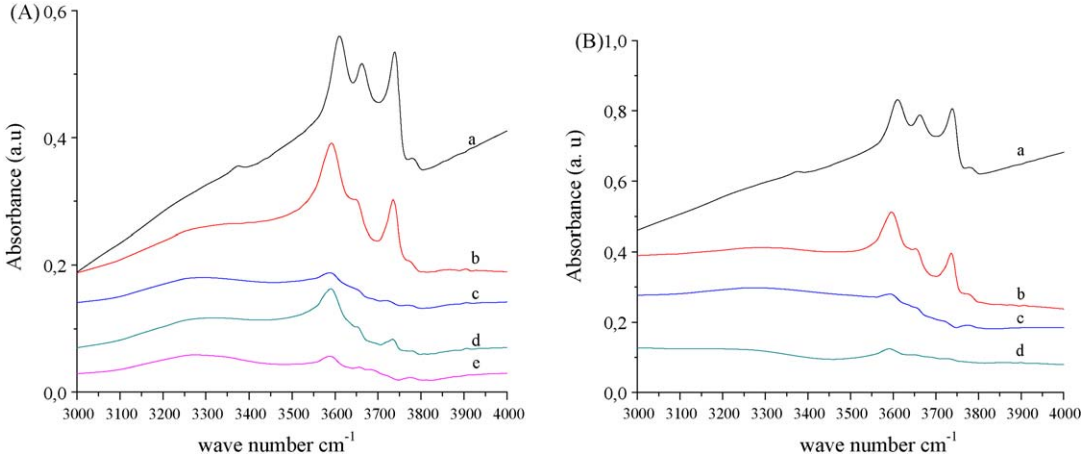

Fig. 2. IR spectra of the OH stretching vibration region of A: (a) H-ZSM-5; (b) V1–Mo2/3–Z; (c) V1–Mo1–Z; (d) V1–Mo4/3–Z; (e) V1–Mo2–Z; B: (a) HZSM-5; (b) V2–Mo2/3–Z; (c) V2–Mo1–Z; (d) V2–Mo2–ZV–Mo–Z.

Table 2
Quantitative analysis of NH_3-TPD (Fig. 4) and of H_2-TPR profiles

Catalysts	NH_3-TPD	H_2-TPR (mmol H_2/g_{cat})		
	Amount of desorbed ammonia (mmol/g)	1st peak (≈600 °C)	2nd peak (≈710 °C)	3rd peak (≈850 °C)
H-ZSM-5(15)	1.01	–	–	–
V1–Z	–	–	0.12	–
Mo1–Z	–	0.82	–	1.03
V1Mo2/3Z	0.62	0.37	–	0.55
V1Mo1Z	0.54	0.73	–	0.99
V1Mo4/3Z	0.45	0.95	–	1.15
V1Mo2Z	0.35	1.16	–	1.44
V2Mo2/3Z	0.46	0.39	–	0.5
V2Mo1Z	0.41	0.62	–	0.72
V2Mo4/3Z	0.32	0.91	–	1.24
V2Mo2Z	0.30	1.26	–	2.42

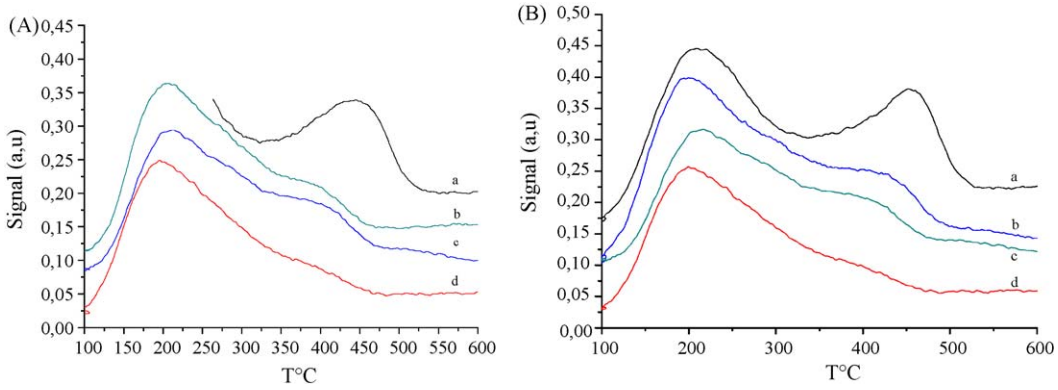

Fig. 3. NH_3 TPD profiles of samples A: (a) V2–Mo2/3–Z; (b) V2–Mo1–Z; (c) V2–Mo4/3–Z; (d) V2–Mo2–Z; B: (a) V1–Mo2/3–Z; (b) V1–Mo1–Z; (c) V1–Mo4/3–Z; (d) V1–Mo2–Z.

3.7. ^{27}Al MAS-RMN

Fig. 4 shows the ^{27}Al MAS NMR spectra of the HZSM-5 and the V–Mo–ZSM-5 catalysts. The ^{27}Al spectrum of the H-ZSM-5 support displayed a main peak at 55 ppm and a weak peak at 0 ppm, corresponding to tetrahedral Al species within zeolite frameworks and octahedral non-framework Al species, respectively [21]. Upon V and Mo essentially loading, the intensities of the peak at 55 ppm dramatically decreased, but the resonance signals at 0 ppm were sharply increased. This suggested that loading of MoO_x distorted the coordination environments of the framework Al species, and some of them might become NMR-invisible due to their lower symmetry [21]. When the molar ratio of Mo increased, the relatively lower peak of tetrahedral framework Al in the samples decreased implied that more MoO_x species interacted with framework Al species. This result is in good agreement with DRIFT spectroscopy and TPD of ammonia. Furthermore the absence of a peak at 14 ppm suggests that no aluminium molybdate $Al_2(MoO_4)_3$ was formed during solid-state ion exchange [22].

3.8. H_2 TPR analysis

H_2 TPR measurements are used to probe the reducibility but may give more information about the nature of vanadium and molybdenum species. The assignment of the TPR peaks is based on the literature study [23–25] and using the reference samples V1–ZSM-5 and Mo1–ZSM-5 prepared by solid-state ion exchange. TPR thermograms of V–Mo–Zeolite systems (Fig. 5) can be divided into three zones of H_2 consumption, corresponding to the reduction of Mo(VI) into Mo(IV), V(V) into V(III) and Mo(IV) into metallic state and seem more like a superposition of both Mo and V-catalysts TPR profiles. TPR profiles of Mo–Zeolite exhibit indeed two reduction peaks at 600 and 850 °C corresponding to the reduction of Mo^{6+} into Mo^{4+} and to the reduction of Mo^{4+} into Mo^0, respectively. On the other hand, V–Zeolite led to a broad asymmetric feature around 710 °C, which has been previously attributed to the reduction of V^{5+} into V^{3+}.

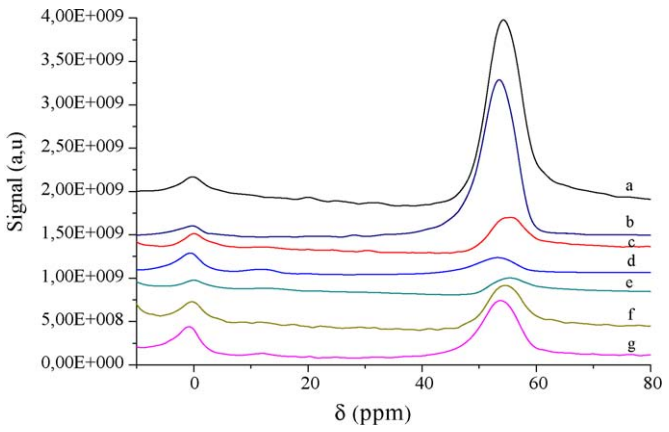

Fig. 4. ^{27}Al MAS NMR spectra of: (a) H-ZSM-5; (b) V2–Z; (c) Mo–Z; (d) V1–Mo1–Z; (e) V1–Mo2–Z; (f) V2–Mo1–Z; (g) V2–Mo2–Z.

3.9. UV–vis spectroscopy

Fig. 6 compares the spectra of V–Mo–ZSM-5 catalysts. The peaks observed at 270 which are assigned to (CT) V–O electron transfer $(\Pi)t_2 \rightarrow (d)e$ and $(\Pi)t_1 \rightarrow (d)e$, respectively for tetrahedrally coordinated and colourless V^{5+} ions transition of the square pyramidally coordinated V species and 300 nm can be attributed to tetrahedral isolated vanadium species [26]. Two overlapped bands at about 215 and 280 nm appeared in all the samples. The absorption at 215 nm represented the Mo=O bond of isolated tetrahedrally molybdate and the absorption at 280 nm could be attributed to the monomer, dimer or polymerized molybdate species [27,28]. The phenomenon suggested that the MoO_x species with different coordination states and local symmetries were dispersed on the HZSM-5 support. Another band at 315 nm is detected and assigned to crystalline MoO_3 phase [29]. The UV–vis spectra of the samples show that no absorption can be observed in wavelength regions longer than 400 nm, indicating that the vanadium species are present as highly dispersed and aggregate vanadium oxide species such as V_2O_5 is not involved in the catalysts.

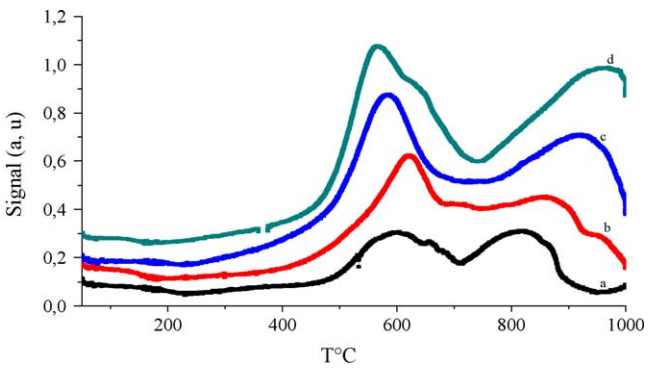

Fig. 5. H_2 TPR profiles of: (a) V1Mo2/3Z; (b) V1Mo1Z; (c) V1Mo4/3Z; (d) V1Mo2Z.

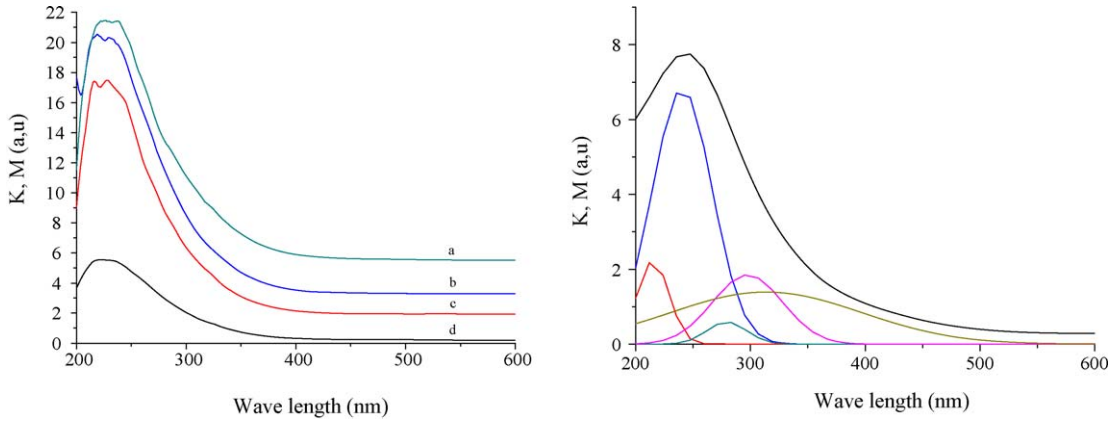

Fig. 6. UV–vis diffuse reflectance spectra of (a) V1–Mo2–Z; (b) V1–Mo4/3–Z; (c) V1–Mo1–Z; (d) V1–Mo2/3Z.

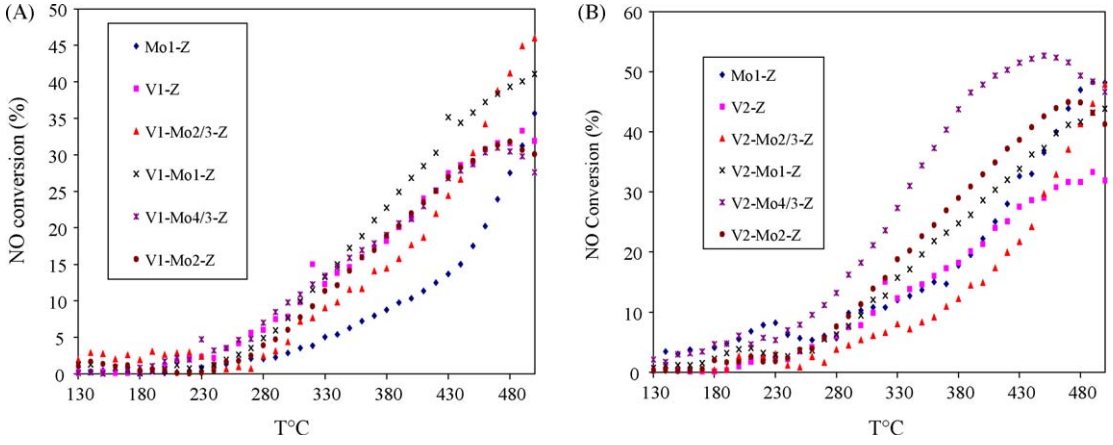

Fig. 7. NO conversion profiles on V1–MoY–Z (A) and V2–MoY–Z (B).

3.10. SCR of NO by NH_3

In Figs. 7 and 8, the catalytic performances of VX–MoY–Z samples are shown as a function of reaction temperature. For the two V–ZSM-5 catalysts, the NO conversion profile remains quite the same and the formation of N_2O is important but does not exceed 250 ppm. On Mo–ZSM–5, the NO conversion is comparable to V–ZSM-5 catalyst if the Molybdenum content is sufficient (2%wt). On these catalysts, the selectivity into N_2 is slightly lower at high temperatures. The addition of Mo to both V1–ZSM-5 and V2–ZSM-5 involves, except for the 2 solids Mo2/3, an increase of the reduction activity of NO with a maximum at Mo content of 8%. But this reduction is not selective since a huge amount of N_2O is formed, particularly in the high temperature region. It is noteworthy that the N_2 selectivity is much higher for the two V–Z catalysts, this probably suggest that Mo, less well dispersed, may contribute to the N_2O formation as reported also by Lietti et al. [30]. It is well known the capability of molybdenum oxide to carry

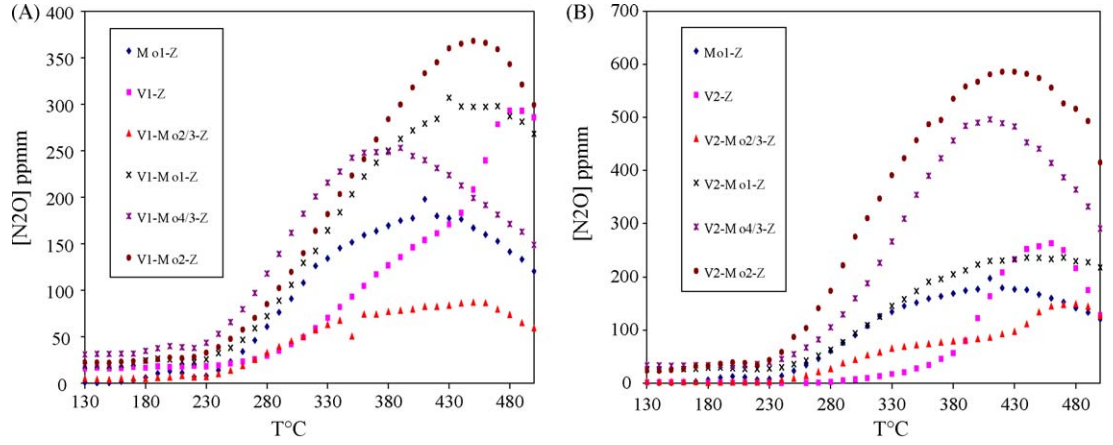

Fig. 8. N_2O formation on V1–MoY–Z (A) and V2–MoY–Z (B) during the SCR reaction.

out the ammonia oxidation reaction. On the contrary, V1–Mo2/3–Z and V2–Mo2/3–Z, although slightly less active, are more selective on the entire temperature window, this behaviour can be explained by the absence of MoO3 which favour the formation of N_2O and the presence of V and Mo species specially in exchangeable sites as suggested by characterization data, which favour the selectivity towards N_2. On the basis of characterization data it has been suggested that the observed synergism in the SCR reaction, for these two solids, is related to the existence of electronic interaction between the V and Mo species, since V and Mo are probably at the exchange sites of the host structure. In particular, it has been proposed that the presence of such electronic interactions modifies the catalysts redox properties, which have been claimed an essential property in the NO-SCR by NH_3 reaction.

4. Conclusion

Solid-state ion exchange of H-ZSM-5 zeolite with both vanadium and molybdenum salts leads to an improved catalyst performance in NO-SCR by NH_3, if the amount of molybdenum added remains low. After solid-state ion exchange, ZSM-5 contains different types of vanadium and molybdenum species depending on the amount of Mo loading: molybdenum in cationic ion exchange position, molybdenum grafted to the silanol groups and molybdenum oxide particles in the channel and/or on the external surface of zeolite. These molybdenum species influence greatly the catalytic properties of the resulting solids.

References

[1] H.G. Karge, H.K. Beyer, Stud. Surf. Sci. Catal. 69 (1991) 43.
[2] A.V. Kucherov, A.A. Slinkin, J. Mol. Catal. 90 (1994) 323.
[3] J.P. Chen, R.T. Yang, Appl. Catal. A Gen. 80 (1992) 135.
[4] L. Lietti, P. Forzatti, F. Bregani, Ind. Eng. Chem. Res. 35 (1996) 3884.
[5] L. Almenay, L. Lietti, N. Ferlazzo, P. Forzatti, G. Busca, E. Giamello, F. Bregani, J. Catal. 155 (1995) 117.
[6] L. Lietti, I. Nova, G. Ramis, L. Dall'Acqua, G. Busca, E. Giamello, P. Forzatti, F. Bregani, J. Catal. 187 (1999) 419.
[7] J. Blanco, P. Avila, C. Barthelemy, A.G. Valdenebro, Appl. Catal. 63 (1990) 403.
[8] H. Matralis, S. Fiasse, R. Castillo, Ph. Bastinas, M. Ruwet, P. Grange, B. Delmon, Catal. Today 17 (1993) 141.
[9] W. Arous, H. Tounsi, S. Djemal, A. Ghorbel, G. Delahay, Top. Catal. 42/43 (2007) 51.
[10] L. Lietti, I. Nova, G. Ramis, L. Dall Acqua, G. Busca, E. Giamello, P. Forzatti, F. Bregani, J. Catal. 187 (1999) 419.
[11] W.G. Klemperer, V.V. Mainz, R.C. Wang, W. Shum, Inorg. Chem. 24 (1985) 1970.
[12] H.Y. Chen, W.M.H. Sachtler, Catal. Today 42 (1998) 73.
[13] El-M. El-Makki, R.A. Van Santen, W.M.H. Sachtler, J. Phys. Chem. B 103 (1999) 4611.
[14] R. Trujillano, J. Grimoult, C. Louis, J.F. Lambert, Stud. Surf. Sci. Catal. 130B (2000) 1055.
[15] W. Li, S.Y. Yu, G.D. Meitzner, E. Iglesia, J. Phys. Chem. B 105 (2001) 1176.
[16] L. Mosqueira, G.A. Fuentes, Mol. Phys. 100 (2002) 3055.
[17] R.W. Borry, Y.h. Kim, A. Huffsmith, J.A. Reimer, E. Iglesia, J. Phys. Chem. B 103 (1998) 5787.
[18] R.R. Pinto, P. Borges, M.A.N.D.A. Lemos, F. Lemos, J.C. Vedrine, E.G. Derouane, F.R. Ribeiro, Appl. Catal. A 284 (2005) 39.
[19] D. Ma, W. Zhang, Y. Shu, X. Liu, Y. Xu, X. Bao, Catal. Lett. 66 (2000) 155.
[20] H. Liu, Y. Li, W. Shen, X. Bao, Y. Xu, Catal. Today 93–95 (2004) 65.
[21] D. Ma, Y. Lu, L. Su, Z. Xu, Z. Tian, Y. Xu, L. Lin, X. Bao, J. Phys. Chem. B 106 (2002) 8524.
[22] J.Z. Zhang, M.A. Long, R.F. Howe, Catal. Today 44 (1998) 293.
[23] K. Chen, S. Xie, A.T. Bell, E. Iglesia, J. Catal. 198 (2001) 232.
[24] K. Chen, A.T. Bell, E. Iglesia, J. Catal. 209 (2002) 35.
[25] N. Steinfeldt, D. Muller, H. Berndt, Catal. Appl. A. 272 (2004) 201.
[26] Z. Wu, H.S. Kim, P.C. Stair, S. Rugmini, S.D. Jackson, J. Phys. Chem. B 109 (2005) 2793.
[27] X. Wang, S. Yu, H. Yang, S. Zhang, Appl. Catal. B 71 (2007) 246.
[28] G. Xiong, Z. Feng, J. Li, Q. Yang, P. Ying, Q. Xin, C. Li, J. Phys. Chem. B 104 (2000) 3581.
[29] A. de Lucas, J.L. Valverde, L. Rodriguez, P. Sanchez, M.T. Garcia, Appl. Catal. A 203 (2000) 81.
[30] L. Lietti, I. Nova, P. Forzatti, Top. Catal. 11/12 (2000) 111.